Investigating the contribution of osteoblastic activity to ADC of bone metastases by correlating changes in ADC with changes in T2* and HU

C. Messiou[1], D. J. Collins[1], M. Robson[2], V. A. Morgan[1], C. Simpkin[1], D. Bianchini[3], J. S. de Bono[3], and N. deSouza[1]

[1]CRUK & EPSRC Cancer Imaging Centre, Institute of Cancer Research & Royal Marsden NHS Foundation Trust, Sutton, Surrey, United Kingdom, [2]Dept. of Cardiovascular Medicine, University of Oxford, Oxford, United Kingdom, [3]Dept. of Medicine, Institute of Cancer Research & Royal Marsden NHS Foundation Trust, Sutton, Surrey, United Kingdom

Introduction: The unique structure of bone marrow presents particular challenges in interpretation of changes in apparent diffusion coefficient (ADC)[1]. Predominantly osteolytic bone metastases have a higher ADC than sclerotic metastases[2] so that ADC is influenced by the balance of osteoblast and osteoclast activity. Magnetic resonance techniques such as ultra short TE (UTE) enable measurement of signal from sclerotic bone and quantified T2* can be used to assess short T2 components within bone metastases[3]. CT Hounsfield units (HU) can also be used as a measure of density of bone metastases. The aim of this study therefore was to investigate the contribution of osteoblastic activity to ADC of bone metastases from prostate carcinoma undergoing treatment by correlating changes in ADC with changes in T2* and HU.

Methods: ***Subjects:*** 16 patients age range 50-83 years (mean age 68.9 years) with histology proven carcinoma of the prostate and bone metastases confirmed on bone scintigraphy or conventional T1W and T2W MRI. ***Imaging protocols:*** Patients were imaged at baseline (within 7 days prior to commencement of therapy) and 12 weeks +/-7 days following commencement of chemotherapy. MRI was performed on a 1.5 T Siemens Avanto using an external coil array with subjects positioned supine. Sagittal T1W (590/11msec TR/TE; 400mmm FOV, 4mm slice thickness) and T2W (2690/93msec TR/TE; 400mm FOV; 4mm slice thickness) images of the spine and axial T1W (607/19msec TR/TE; 340mm FOV; 5mm slice thickness) and T2W (5340/127msec TR/TE; 340 mm FOV; 5mm slice thickness) images of the pelvis were acquired. Axial single shot twice refocused diffusion weighted spin echo planar images[4] were acquired covering the lumbar spine and pelvis with the following parameters: 3000/80msec TR/TE; FOV 350 mm, slice thickness 5mm, 4 averages, 3 orthogonal directions and b values of 0, 50, 100, 250, 500 and 750 smm^{-2} with SPAIR fat saturation. Sagittal and axial 2D UTE of the lumbar spine and pelvis was also performed: TR 500ms, FOV 800mm, matrix 512, 4 averages, flip angle 85º, BW 540Hz, fat saturation; 4mm slice thickness, spine elements 5, 6 and 7 and body coils 1 and 2 with TEs 0.07, 7.4 and 9.4ms and 4 averages. CT of the chest, abdomen and pelvis was performed as part of routine clinical staging : GE Lightspeed (GE Healthcare Technologies, Waukesha, WI): Omnipaque 300 100mls at 3ml/s portovenous phase using a Smartprep technique, 16 slice, 1.25mm thick with 5mm reconstructions. ***Data Analysis***: Monoexponential ADC maps using all 6 b values (0, 50,100, 250, 500, 750 smm^{-2}) were generated using system software taking an average value for the 3 directions of diffusion sensitisation. ADC maps were also generated using b 100, 250, 500, 750 smm^{-2} (ADCslow). Using T1W MR sequences to aid ROI placement up to 5 regions of interest (ROIs) were drawn around lesions on ADC maps avoiding artefacts. T2* maps were generated using Diffusionview software with a monoexponential fit over 3 echo times. Lesions corresponding to those chosen for DWI analysis were selected and ROIs were drawn on the T2* maps avoiding artefacts. Axial CT images and multiplanar reformats of the lumbar spine and pelvis generated using a bone algorithm were viewed in conjunction with all MRI imaging. Lesions corresponding to those chosen for DWI/T2* analysis were selected. ROIs were drawn on axial images or sagittal reformats as appropriate to correspond with lesions analysed on DWI/UTE imaging. All measurements were made on baseline scans and on the corresponding lesions on the 12 week follow up scans. ***Statistics:*** Data were analysed using SPSS (v15) and tested for normality using the Kolmogorov-Smirnov test. Correlations between changes in ADC and T2* and HU were investigated using a Pearson's correlation coefficient.

Results: Mean ROI area of all bone lesions at baseline was 8.0 +/- 4.0 cm^2. Corresponding pre and post treatment ADC and HU were available on 60 lesions from 16 patients. Corresponding pre and post treatment ADC and T2* were available on 12 lesions from 6 patients.

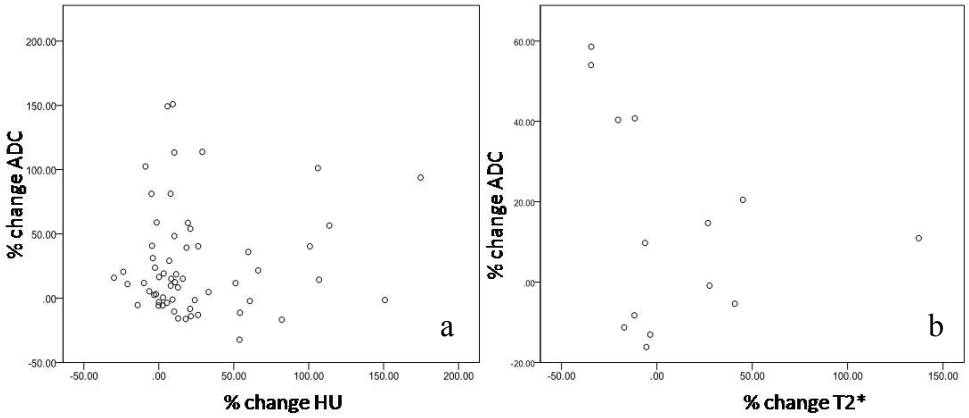

Figure 1. Percentage change in ADC ($x10^{-6}mm^2s^{-1}$) vs mean HU (a) and percentage change ADC ($x10^{-6}mm^2s^{-1}$) vs percentage change in T2* (b) show no significant correlation with Pearson correlation coefficients of 0.721 and 0.343 respectively. Plots using % change in ADCslow produced similar results.

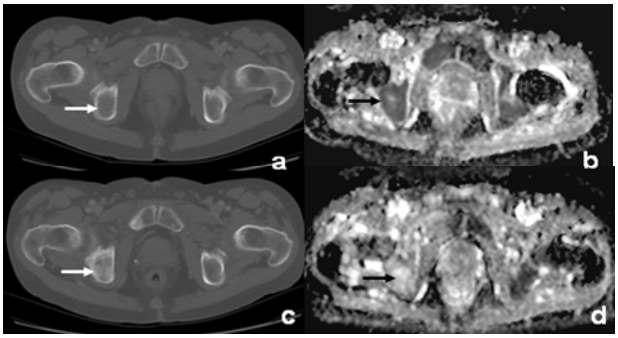

Figure 2. The relationship between ADC ($x10^{-6}mm^2s^{-1}$) and HU. Axial CT bone windows of the pelvis and corresponding ADC map pre (a and b) and 12 weeks post chemotherapy (c and d) in a patient with bone metastases secondary to carcinoma of the prostate. The metastatic deposit in the right ischial tuberosity (a, arrow) shows sclerotic healing after treatment (c, arrow) with an increase in HU from 142 to 390HU, as the patient responds to treatment (PSA fell from 84 to 23.9 ng/ml). Corresponding ADC maps show that ADC has risen from 877 to $1700mm^2s^{-1}x10^{-6}$ despite the increase in bone sclerosis (b and d arrows).

Conclusion: Percentage changes in ADC did not correlate with percentage change in HU or T2*. This may be because intertrabecular distance is beyond the range interrogated by the DWI technique employed in this study and does not affect the ADC measurement. High resolution CT studies indicate a normal intertrabecular distance of anywhere between 2.63 and 5.3mm depending on age and sex (5,6). Intercellular distances however are of the order of μm. Because intertrabecular distance is so large relative to cell size, a marked sclerotic response may be required to bring intratrabecular distances down to a level where it affects intercellular distances and diminishes ADC.

References: 1. Messiou C et al Cancer Biomarkers 2010 ;6:21-32; 2. Messiou et al ISMRM 2009: 3943; 3.Messiou et al ISMRM 2009: 4004; 4. Reese et al. MRM 2003 49(1):177-82; 5. Park SH et al J Shoulder Elbow Surg 2009 19(2):244-50; 6. Mundinger A et al Br J Radiol 1993 66(783):209-13.